

# STRUCTURAL DAMAGE IDENTIFICATION USING MATHEMATICAL OPTIMIZATION TECHNIQUES

Mo-How Herman Shen

Department of Aeronautical and Astronautical Engineering  
 The Ohio State University

N92-13936

p. 12

## Abstract

An identification procedure is proposed to identify the damage characteristics (location and size of the damage) from dynamic measurements. This procedure was based on minimization of the 'mean-square' measure of difference between measurement data (natural frequencies and mode shapes) and the corresponding predictions obtained from the computational model. The procedure is tested for simulated damage in the form of stiffness changes in a simple fixed-free spring-mass system and symmetric cracks in a simply-supported Bernoulli-Euler beam. It is shown that when all the mode information were used in the identification procedure it is possible to uniquely determine the damage properties. Without knowing the complete set of modal information, a restricted region in the initial data space has been found for realistic and convergent solution from the identification process.

## Introduction

There is a considerable body of research on identification problems, that is, the problem of identifying the engineering properties or reconstructing the structural configuration of a vibrating system from certain natural frequency spectra and/or corresponding mode shape. Such problems were considered by Barcilon [1, 2], McLaughlin [3, 4], Gladwell [5-7], and Gladwell *et al.* [8]. Most of these studies involve the determination of material properties from natural frequencies, and they emphasize the existence, uniqueness, and methods for determination of properties (termed 'reconstruction').

An detection procedure was developed by Shen and Taylor [9] to determine the crack characteristics (location  $xc$  and size  $cr$  of the crack) of Bernoulli-Euler beams from their dynamic response. The idea of this procedure was related to methods of structural optimization. Specifically, the structural damage was identified in a way to minimize one or another measure of the difference between a set of data (measurements)  $T_d$ , and the corresponding values for dynamic response  $M_d$  obtained by analysis of a model for the damaged beam. This may be expressed symbolically as the following optimization problem:

$$\min_{xc, cr} \text{norm}(T_d - M_d). \quad (1)$$

Naturally, the minimization represented here is constrained by the equations which model the physical system. Moreover, as indicated in the discussion by Shen and Pierre [10, 11], one can note that the more modal information used for crack detection, the more accurate and reliable the result that can be achieved. For practical purposes, the objective of Eq. (1) was formulated based on a certain set of specific modes; specifically the first three modes are considered in the inverse procedure.

In this study the corresponding to the mean-square measure of the norm, as shown in Eq. (1), is examined. The identification process is based on minimization of the 'mean-square' measure of difference between measurement data (natural frequencies and mode shapes) and the corresponding predictions obtained from the computational model. The identification procedure is tested for

simulated damage in the form of a symmetric cracks in a simply-supported Bernoulli-Euler beam and a fixed-free spring-mass model. The uniqueness and reliability of the identification process is confirmed by solving several damage identification examples with specified damage positions.

## Problem Statement

In this section, variational formulations for the identification of damaged one-dimensional structures are presented. The mean square differences between measured and modeled values of frequency and mode shape are employed as the objective function in one of the formulations. In other words, the inverse process seeks to determine the damage parameters, location  $xc$  and size  $cr$ , in the mathematical model to minimize the mean square difference between the test data and analytical predictions. The problem formulations are presented in forms of a cracked Bernoulli-Euler beam and a multi degrees of freedom (DOF) spring-mass system.

### Cracked beam model

In the treatment of this problem, it is assumed that the testing information (data) is provided from certain test points distributed over the structure. This data is comprised of frequency and mode shape information associated with the lower several response modes.

For a simply-supported uniform beam containing one pair of symmetric cracks (see Fig. 1), the problem of optimization in crack detection can be expressed, in terms of comparisons between modeled response and test data, as

$$\min_{cr, xc} [norm(\omega_{t\alpha}^2 - \omega_{\alpha}^2, w_{t\alpha}(x_{tm}) - w_{\alpha}(x_{tm}))] \quad (2)$$

subject to constraints that define the beam response  $w_{\alpha}$  (ie., the equations for free vibration), and which prescribe appropriate normalization of  $w_{\alpha}$  and test data  $w_{t\alpha}$ .

Here  $cr = \frac{d-h}{d}$  represents crack ratio (a measure of crack depth), and  $xc$  identifies crack position (see Fig. 1). Also, the objective function measure of differences between measured and modeled values of deflection and frequency in Eq. (2) is stated for present purposes in the form:

$$norm(\omega_{t\alpha}^2 - \omega_{\alpha}^2, w_{t\alpha} - w_{\alpha}) = \left( \sum_{\alpha=1}^M [(\omega_{t\alpha}^2 - \omega_{\alpha}^2)^2 + \sum_{m=1}^T (w_{t\alpha}(x_{tm}) - w_{\alpha}(x_{tm}))^2] \right)^{\frac{1}{2}} \quad (3)$$

where  $\omega_{\alpha}$ ,  $w_{\alpha}$  represent the natural frequency and mode shape of  $\alpha$ th bending free vibration mode,  $M$  is the number of modes for which test information is available, and, once again, the corresponding test data are symbolized by  $\omega_{t\alpha}$  and  $w_{t\alpha}$ . Here  $x_{tm}$  ( $m = 1, 2, \dots, T$ ) locates the  $m$ -th out of  $T$  measure stations, respectively. The measures  $w_{t\alpha}$  and  $w_{\alpha}$  that appear in the norm must be normalized on a common basis in order to facilitate comparison between the data and model values.

The symbol  $\Phi$  is introduced to represent the square of the norm given in Eq. (3). The identification problem now can be stated:

$$\min_{cr, xc} \Phi \quad (4)$$

subject to:

$$\int_0^l \{EIQ(w_{\alpha}''(x))^2 - \omega_{\alpha}^2 \rho A w_{\alpha}^2(x)\} dx = 0 \quad (5)$$

$$\sum_{m=2}^{T-1} (w_{\alpha}(x_{tm}) w_{\beta}(x_{tm})) \Delta x_{tm} - \eta_{\alpha\beta} = 0 \quad (6)$$

$$(cr + \underline{a} xc) - R \leq 0 \quad (7)$$

$$\underline{cr} \leq cr \leq \overline{cr} \quad (8)$$

$$\underline{xc} \leq xc \leq \overline{xc} \quad (9)$$

where  $\alpha, \beta=1, \dots, M$ ,  $\underline{a}$  is a weighting factor on the  $cr$  and  $xc$ ,  $R$  represents the upper bound on value  $cr + \underline{a}xc$ , and  $\overline{xc}$ ,  $\underline{xc}$ , and  $\overline{cr}$ ,  $\underline{cr}$  represent the upper and lower bounds of the crack (damage) parameters  $xc$  and  $cr$ , respectively. (Note that both upper and lower bounds on the variables  $cr$  and  $xc$  are necessary in the present problem.) Since  $w_\alpha$  comprise an orthonormal set,  $\eta_{\alpha\beta}$  is defined as

$$\eta_{\alpha\alpha} = \sum_{m=2}^{T-1} w_\alpha^2 |x_{tm}| \Delta x_{tm}, \quad \lim_{T \rightarrow \infty} \eta_{\alpha\beta} = 0 \quad \text{for } \alpha \neq \beta \quad (10)$$

The effect of cracks on the structural properties of the beam is reflected by factor  $Q$  in Eq. (5), as described for symmetric surface cracks in Shen and Pierre [10]. In other words, the optimization parameters  $xc$  and  $cr$  cited in Eq. (4) enter the problem via  $Q$ .

According to the K-K-T (Kurash-Kuhn-Tucker) necessary conditions for the optimization problem Eqs. (4-9), there exist Lagrange multipliers  $\lambda_\alpha$ ,  $\Lambda_{\alpha\beta}$ , and  $\Gamma_k$  which satisfy the following equations (the notation ' $|_*$ ' refers to solution points):

$$\lambda_\alpha > 0$$

$$\Lambda_{\alpha\beta} > 0$$

$$\Gamma_1 [(cr + \underline{a}xc) - R] |_* = 0 \quad (11)$$

$$[\Gamma_2 (\underline{cr} - cr)] |_* = 0 \quad (12)$$

$$[\Gamma_3 (xc - \overline{xc})] |_* = 0 \quad (13)$$

$$[\Gamma_4 (\underline{xc} - xc)] |_* = 0 \quad (14)$$

$$[\Gamma_5 (cr - \overline{cr})] |_* = 0 \quad (15)$$

The solution must satisfy the following three equations as well:

$$[2(\omega_{i\alpha}^2 - \omega_\alpha^2) + \lambda_\alpha \rho A C_\alpha^2] |_* = 0 \quad (16)$$

$$[(EIQw_\alpha''(x))'' - \omega_\alpha^2 \rho A w_\alpha(x)] |_* = 0 \quad ; x_{tm} < x < x_{t(m+1)} \quad (17)$$

$$\begin{aligned} & \sum_{m=2}^{T-1} \{-2(w_{i\alpha}(x) - w_\alpha(x)) + [2\Lambda_{\alpha\alpha} w_\alpha(x) + \sum_{\beta=1}^{\alpha-1} \Lambda_{\alpha\beta} w_\beta(x) \\ & + \sum_{\beta=\alpha+1}^M \Lambda_{\alpha\beta} w_\beta(x)] \Delta x_{tm} + 2\lambda_\alpha [(EIQw_\alpha''(x))'' - \omega_\alpha^2 \rho A w_\alpha(x)]\} |_{x=x_{tm}} |_* = 0 \end{aligned} \quad (18)$$

Note that the above equation of motion (Eq. 17) is valid interval by interval over the span of the structure.

Finally, the conditions for stationarity of  $\Phi$  w.r.t. the optimization variables  $cr$  and  $xc$  (ie., the optimality conditions) are:

$$\left[ \sum_{\alpha=1}^M \lambda_\alpha (EI \int_0^l \frac{\partial Q}{\partial cr} (w_\alpha''(x))^2 dx) + \Gamma_1 - \Gamma_2 + \Gamma_5 \right] |_* = 0 \quad (19)$$

$$\left[ \sum_{\alpha=1}^M \lambda_{\alpha} (EI \int_0^l \frac{\partial Q}{\partial x c} (w_{\alpha}''(x))^2 dx) + \Gamma_1 \underline{a} + \Gamma_3 - \Gamma_4 \right] |_{*} = 0 \quad (20)$$

• *The problem formulation for the numerical method-mean square criterion*

The purpose in this subsection is to re-state the inverse cracked beam problem with mean square criterion, Eqs. (4-9), in the following form that is more convenient for computational purposes. With the introduction of symbols  $\xi$  and  $\Upsilon$  for convenience, the statement becomes:

$$\min_{\underline{x}_1} \sum_{\alpha=1}^M [(\xi_{t\alpha} - \xi_{\alpha})^2 + \sum_{m=1}^T (w_{t\alpha}(x_{tm}) - w_{\alpha}(x_{tm}))^2] \quad (21)$$

subject to :

$$[\alpha^4 Q \sum_{m=1}^T (w_{\alpha}(x_{tm}))^2 - \xi_{\alpha} \sum_{m=1}^T (w_{\alpha}(x_{tm}))^2] \Delta x_{tm} - \Upsilon_{\alpha} = 0 \quad (22)$$

$$\sum_{m=2}^{T-1} (w_{\alpha}(x_{tm}) w_{\beta}(x_{tm})) \Delta x_{tm} - \eta_{\alpha\beta} = 0 \quad (23)$$

$$0 \leq cr \leq 1.0 \quad (24)$$

$$0 \leq xc \leq 1.0 \quad (25)$$

where  $\alpha, \beta = 1, \dots, M$ , variable vector  $\underline{x}_1 = \{cr, xc, \xi_{\alpha}, w_{\alpha}(x_{tm})\}$ ,

$$\xi_{\alpha} = \frac{\omega_{\alpha}^2 l^4 \rho A}{EI \pi^4} \quad (26)$$

and

$$\Upsilon_{\alpha} = [\alpha^4 Q \sum_{m=1}^T (w_{t\alpha}(x_{tm}))^2 - \xi_{\alpha} \sum_{m=1}^T (w_{t\alpha}(x_{tm}))^2] \Delta x_{tm} \quad (27)$$

**Spring-mass model**

The spring-mass model to which the present identification procedure is applied is shown in Fig. 2. It consists of 3 masses connected by linear springs of stiffness defined by

$$k_i = k(1.0 - \frac{dm_i}{3})^3 \quad (28)$$

where  $dm_i$  is defined as a damage parameter at  $i$ -th spring. If  $dm_i$  is interpreted to represent the same physical meaning as  $cr$  does in the cracked beam model, the system's damage condition may be introduced by specifying a certain value to 'damage parameters'. For instance, according to Eq. (28), a damaged condition can be constructed in which stiffness drops 25% and 50% at the spring 2 and 3. This is accomplished by assigning the values  $dm_2$  and  $dm_3$  to be 0.2743 and 0.6189, respectively. In a sense, the spring-mass model can be viewed as a simple simulation analogy of the cracked beam, ie., both extent and location of damage can be represented in the model. The fundamental frequencies  $\omega_i$  of axial vibrations are related to the mode shapes  $\tilde{u}_i = (u_1, u_2, u_3)_i^T$ ,  $i = 1, 2, 3$  through the equations:

$$\tilde{u}_i^T [K_s] \tilde{u}_i - \xi_i \tilde{u}_i^T [I] \tilde{u}_i = 0 ; i = 1, 2, 3 \quad (29)$$

where  $\xi_i = \frac{m\omega_i^2}{k}$ . Therefore, the present damage identification problem can be stated as

$$\min_{\underline{x} = dm_i, \xi_i, \tilde{u}_i} \sum_{i=1}^3 [(\xi_{ti} - \xi_i)^2] + \sum_{j=1}^3 (\tilde{u}_{tji} - \tilde{u}_{ji})^2 \quad (30)$$

subject to:

$$\tilde{u}_i^T [K_s] \tilde{u}_i - \xi_i \tilde{u}_i^T \tilde{u}_i = 0 \quad ; i = 1, 2, 3 \quad (31)$$

$$\tilde{u}_i^T \tilde{u}_j - \delta_{ij} = 0 \quad ; i, j = 1, 2, 3 \quad (32)$$

$$0 \leq dm_i \leq 1.0 \quad (33)$$

## Numerical Analysis

The numerical optimization technique set forth in this study for vibrating cracked beam identification problems is accomplished using the VMCON optimization package program (this implements a sequential quadratic programming method). The VMCON program uses Powell's algorithm which is an iterative scheme designed to converge to a point that satisfies the necessary conditions. Additional information regarding to VMCON is available in Ref. [12].

### Cracked beam model

The cracked beam model to which the identification procedure is applied is shown in Fig. 1. It is a simply supported beam of length  $l$  equal to 18.11 of it's thickness  $2d$ , with uniform rectangular cross-section area  $A$ , and a pair of symmetric cracks of  $cr = 0.5$  located at mid-span ( $xc = 0.5$ ).

Unless otherwise stated, the damage properties ( $cr$  and  $xc$ ) of the simply supported cracked beams are identified by direct solution of the optimization problems described in the previous section. The sensitivity to chosen values for the initial crack position  $xc$  are discussed later in this section.

#### • *Examples with position of the crack (damage) specified*

Consider the first example for crack identification, the simply supported cracked beam, for which the crack position  $xc$  is known. In other words, only the crack ratio  $cr$  is to be identified; therefore, the variables in this problem are  $cr$ ,  $\xi$ 's, and mode shapes  $w_\alpha(x)$  ( $\underline{x}_1 = \{cr, \xi_\alpha, w_\alpha(x_{tm})\}$ ,  $\underline{x}_2 = \{cr, \xi_\alpha, a_{\alpha i}\}$ ). This simplified example problem with the crack position specified ( $xc = 0.5$ ) is presented to demonstrate the concept of the crack identification procedure described in the last section.

In this example, it is assumed that the dynamic measurements are collected at 9 test positions ( $T = 9$ ) equally spaced over the span. The first and last test stations are located at the left and right supported end, respectively. Hence, the length of each test span  $\Delta x_{tm}$ ,  $m = 1, \dots, T - 1$  is determined to be  $\frac{36.22d}{T-1}$ . In structural dynamic testing, ordinarily only a relatively small subset of the theoretically available eigenvalues and eigenvectors can be measured accurately, i.e., realistic information on higher modes is difficult to obtain from the measurements at a limited set of test stations. Only information from the first three modes is to be used as test data in the present identification process. Furthermore, according to the observations in Shen and Pierre [10], the even modes of a simply supported beam are not sensitive to a mid-span crack; therefore, in effect only first and third mode ( $\alpha = 1, 3$ ) information is used to represent crack damage.

Once again, the crack identification problem presented by Eqs. 21-25 is solved here with a specified value  $xc = 0.5$ . For given initial values of  $\underline{x}$ , this optimization problem is solved to minimize the criterion  $F$ . The results of the cases with various initial conditions are shown in Table 1. In order to clearly compare the results, only the first three variables,  $\xi_1, \xi_3, cr$ , of variable vector  $\underline{x}_1$  are listed in the Table 1.

In Table 1, the top row denotes the assumed crack ratio and corresponding first and third eigenfrequencies. The symbol \* denotes the expected optimal solution through the identification process. The first two column entries,  $\xi_1, \xi_3$ , indicate the fundamental and the third frequencies corresponding to the initial crack ratio  $cr$  which is given in the next column. The last three columns give the final values corresponding to previous entry values. These final values are obtained at the

stage where computation is terminated when the further optimal search obtains improvements for criterion  $F$  less than the specified tolerance ( $10E - 5$  was adopted in the present study). Recall that for an uncracked beam  $cr$  is identically zero. Therefore, in this example, it is decided to start with the case of the initial value  $cr = 0.0$  and for each case thereafter the  $cr$  value is increased by 0.1.

From the results presented in the first case of Table 1, one sees that the parameters  $\xi_1, \xi_3$ , and  $cr$  were identified to be 0.84684, 70.1348, and 0.50033 from 1.0, 81.0, and 0.0, respectively. The mean square criteria  $F$  was cut down from 118.13502 to 0.42440E-5. The maximum error is less than 0.5% of the test data for these parameters. The results are also quite impressive for mode shapes. In order to observe the global variance clearly, the initial, final, and testing mode shapes are plotted in Fig. 3. Three curves appear on each plot: the initial mode shape, the final mode shape, and the mode shape from test response. The final mode shape on these plots agrees well with the test mode shape. This is expected and verified the accuracy observed from the results in Table 1. It can be clearly seen that accuracy of the mode shapes will worsen if higher mode results are to be predicted. Improvement can be obtained by an appropriate adjustment of the location of these test stations. However, a sensitivity analysis of the test stations with respect to the accuracy of the dynamic measurements is required. This is not considered further in the present study.

In Table 1, rows 5 to 11 present the results for cases with initial  $cr = 0.1$  to 0.8. The corresponding final point values listed in the columns 4-6 show that these cases exhibit, as expected, similar solution characteristics and accuracy. This provides a physical understanding of the geometry of the solution set: for the inverse cracked beam problem with specified crack position, the mean square criterion of Eq. (21) is a convex function and it is bounded by the constraints of Eqs. (22-25). Hence, one may conclude that the convergence of the present optimization problem is obtained independent of the initial data chosen. In other words, as long as the initial data is selected within the problem's feasible domain, an accurate and unique solution through the identification process is expected.

Clearly the prediction of mode 3 shape shown in Fig. 3 fails to reproduce the expected sin curve. This is because the 3rd mode shape was plotted based on the deflections of the mode shape measured at only 9 test stations. While this reflects a limitation on how well mode shapes are portrayed, the quality of the final result for the identification problem is unaffected.

#### • *Simultaneous identification of crack position and depth*

The second numerical example deals with the crack identification of a simply supported cracked beam with unknown crack ratio and with crack position unknown. In this treatment, the variables in the optimization problem are  $cr, xc, \xi$ 's, and mode shapes  $w_\alpha(x)$  ( $\underline{x}_1 = \{cr, xc, \xi_\alpha, w_\alpha(x_{tm})\}$ ). Due to the limitations of the VMCON program, the examples that concerning with the testing mode shapes  $w_t$  provided in the form of continuous functions are not shown in this subsection.

The formulation of the crack identification problem (Eqs. 21-25) is tested again with both crack position and depth are assumed unknown. In the first few cases, the simulated dynamic test measurements are assumed to be collected at 9 equally spaced test stations ( $T = 9$ ). The first and last test positions are located at the left and right supported end, respectively. This example will be solved a second time using an increased number of test stations, to provide information on sensitivity of the procedure to the amount of test data.

In Table 2, the top row denotes the assumed crack ratio, crack position, and corresponding first and third eigenfrequencies. The symbol \* denotes the expected optimal solution through the identification process. The first column entry  $T$  denotes the number of test stations used to collect dynamic measurements. The second and third column entries,  $\xi_1, \xi_3$ , indicate the fundamental and the third frequencies corresponding to the initial crack ratio  $cr$  and crack position  $xc$ , which are given in the next two columns. The last four columns provide the final values corresponding to

the previous entry values. These final values are obtained at the stage where the computation is terminated, when the optimal search obtains step-wise improvements of  $F$  less than a specified tolerance ( $10E-5$  in the present study).

Table 2 shows that cases with  $T=9$  have the final values of  $\xi$  close to  $\xi^*$ , but almost all of these cases have unacceptable final estimates of  $xc$  and  $cr$ . For instance, if the initial position is selected as  $xc = 0.4$  and  $cr = 0.4$ , the values of  $xc$  and  $cr$  at the final iteration are 0.99789 and 0.36289 which are approximately 98% and 28% different than the given test data. In other words, evidently the configuration with  $xc = 0.99789$  and  $cr = 0.36289$  is able to provide another minimum value of the criterion (besides the one associated with the expected result). This cracked beam configuration is shown in the solid curve of Fig. 4. The mis-match between final and test mode shapes can be clearly seen. This observation confirmed the unacceptable error previously obtained in the comparison of  $xc$  and  $cr$  between the final and test data. Except for the case with initial  $cr = 0.4$  and  $xc = 0.48$  which provides less than 1% estimation error, the rest of the cases in Table 2 with 9 test stations are also found to have similarly large estimation error. Therefore a dependable solution in crack identification is almost impossible to achieve on the basis of the 9 test stations simulated measurement information on first and third mode response. This confirmed the observations in Shen and Pierre [10, 11], i.e., for a cracked beam with an unknown crack position, a unique solution is not to be expected.

However, by comparing the third mode shape in Figs. 3(b) and 4(b) to the mode shape in Fig. 11(c) of Ref. [10], it can be seen that an accurate third mode shape can not be approximated based on the displacements collected from 9 test stations only. This implies that the accuracy of the above computational identification might be improved if the third mode is approximated well. Therefore, the cases with more test stations should be examined since they would clearly provide better mode shape approximation. The largest number of test stations which can be accommodated in the identification procedure is 45, due to the limitations of the optimization program package. Once again, the test measurement points are equally spaced, and first and last stations are set located at the left and right supported end, respectively. The VMCON problem formulation is identical to the case of  $T=9$ ; however, the variable vector  $\underline{x}$  is expanded from 22 components to 94.

Rows 12 to 17 of Table 2 summarizes the results through the minimization process. As in the previous cases, the final values of frequency  $\xi$  are observed to be close to test values  $\xi^*$ . Acceptable final solution values for  $xc$  and  $cr$  are shown in the results of the cases in which initial  $xc$  and  $cr$  are selected within the range from  $xc = 0.4, cr = 0.4$  to  $xc = 0.6, cr = 0.6$ . On the other hand, within this range, good agreement is also shown in mode shapes. Figures. 5 and 6 display the initial, final, and test mode shapes for cases with the initial  $xc = 0.4, cr = 0.4$  and  $xc = 0.6, cr = 0.6$ . Excellent agreement is observed between the final and test mode shapes. Moreover, by comparing the final data curve in Figs. 5 and 6 with the mode shape in Fig. 11(c) of Ref. [10], a more accurate third mode is approximated. This indicates that more accurate information on mode shapes is required to obtain a satisfactory solution from the identification process in the case where both crack position and crack depth are unknown.

Questions arise concerning the conditions under which the identification procedure can provide a unique solution. As discussed in Shen and Pierre [10, 11] and concluded in the studies of Gladwell *et. al.* [8], if all the mode information is used in the identification procedure, then the system's properties can be identified uniquely. However, for practical reasons, in structural dynamic testing only a small subset of the eigenvalues and eigenvectors can be represented in the measurement data. Furthermore, even if substantially more modal information would be available, the minimization search may be prohibitive for such a large-dimensional feasible domain that would result. These comments are intended to point out certain limitations inherent in the identification procedures. These considerations is addressed with the presentation in the following, which

describes sufficient conditions for the unique identification from the dynamic measurements of a multi DOF vibrating spring-mass system.

### **Spring-mass model**

The following examples of damage identification problems were constructed by introducing the damage through the drop in the stiffness or, more conveniently, the value of each damage parameter to change the system's dynamics behaviour. These dynamic changes, taken as the test simulation of response data, are used to deduce the value of each damage parameter via the identification process.

The numerical optimization technique set forth in this study for vibrating cracked beam identification problems is accomplished using the VMCON optimization package program (this implements a sequential quadratic programming method). The damage properties ( $dm_i, i = 1, 2, 3$ ) of the fixed-free spring-mass system are identified by direct solution of the optimization problems described in the previous section.

The first example corresponds to the identification of a system's damage,  $dm_1 = 0.0, dm_2 = 0.5, dm_3 = 0.25$ , using first and second mode information. The first five variables,  $\xi_1, \xi_2, dm_1, dm_2$ , and  $dm_3$  of each vector  $\underline{x}$  are listed in Table 3. The top row denotes the assumed damage parameters and corresponding first and second eigenfrequencies and the symbol \* denotes the expected optimal solution through the identification process. The first and second column entries,  $\xi_1, \xi_2$ , indicate the fundamental and the second frequencies corresponding to the initial damage parameters,  $dm_1, dm_2, dm_3$ , which are given in the next three columns. The last five columns give the final values corresponding to previous entry values. These final values are obtained at the stage of the program is terminated when the further optimal search obtain improvements  $F$  less than a tolerance ( $10E - 5$  was adopted in the present study).

In Table 3, each case has the final values of  $\xi$  close to  $\xi^*$ , but almost all of them have the unacceptable final results for  $xc$  and  $cr$ . Only the case with initial  $dm_2 = 0.48$  and  $dm_3 = 0.24$  has less than a 1% estimation error. These results show performance of the present damage identification process is generally unacceptable if only first and second modes are used.

The first six variables,  $\xi_1, \xi_2, \xi_3, dm_1, dm_2$ , and  $dm_3$  of each vector  $\underline{x}$  are listed in Table 4 the top row denotes the assumed damage parameters and corresponding first and second eigenfrequencies and the symbol \* denotes the expected optimal solution through the identification process. In this example, all the modes are used to deduce the damage conditions. Satisfactory predictions are obtained in each case, in contrast to the results examined in Table 3. Even though starting point is located at boundary of the feasible set ( $dm_1 = 0.0, dm_2 = 0.0, dm_3 = 0.0$ ), the agreement is still precise. These results confirm the expectation that a unique and accurate solution predictions are assured if all the modal information is included as data in the damage identification process.

## **Conclusions**

A general method for damage identification of a simple beam and a spring-mass system is presented. The method may be useful as a component of an on-line nonintrusive damage detection technique for vibrating structures. A formulation is expressed as a direct minimization problem statement with a criteria of the mean square difference of natural frequencies and mode shapes between test measurements and corresponding model values. The damage identification problem is reduced to finding the damage parameters that will satisfy appropriate constraints and minimize the mean square difference.

The uniqueness and reliability of the identification process is confirmed by solving several damage identification examples with specified damage positions. Without knowing the damaged location, a restricted region in initial data space had been found for which there will be a realistic



and convergent solution from the identification process. This region is small, and can be expanded if substantially more modal information would be available. However, the minimization search may be prohibitive for such a large-dimensional feasible domain that would result.

## References

- [1] V. Barcilon 1976 *Zeitschrift Fuer Angewandte Mathematik Und Physik* **27**, 346-358. Inverse Problem for a Vibrating Beam.
- [2] V. Barcilon 1982 *Philosophical Transactions of the Royal Society of London* **304**, Ser. A, 211-252. Inverse Problems for the Vibrating Beam in the Free-Clamped Configuration.
- [3] J. R. McLaughlin 1984 in Santosa, F., Symes, W. W., Pao, Y. H., and Holland, C., (Eds.), *Inverse Problems of Acoustic and Elastic Waves*, SIAM, 341-347. On Constructing Solutions to an Inverse Euler-Bernoulli Beam Problem.
- [4] J. R. McLaughlin 1986 *SIAM Review* **28**, 53-72. Analytical Methods for Recovering Coefficients in Sturm-Liouville Equations.
- [5] G. M. L. Gladwell 1984 *Proceeding of the Royal Society of London* **393**, Series A, 277-295. The Inverse Problem for the Vibrating Beam.
- [6] G. M. L. Gladwell 1985 *Proceeding of the Royal Society of London* **401**, Series A, 299-315. Qualitative Properties of Vibrating Beam.
- [7] G. M. L. Gladwell 1986 *Proceeding of the Royal Society of London*, **407**, Series A, 199-218. The Inverse Problem for the Euler-Bernoulli Beam.
- [8] G. M. L. Gladwell, A. H. England, and D. Wang 1987 *Journal of Sound and Vibration* **119**, 81-94. Examples of Reconstruction of an Euler-Bernoulli Beam from Spectral Data.
- [9] M. H. Shen and J. E. Taylor, *Journal of Sound and Vibration* **150**, NO.1, October 1991. An Identification Problem for Vibrating Cracked Beams.
- [10] M. H. Shen and C. Pierre, 1990 *Journal of Sound and Vibration* Vol. 138, No. 1, pp. 115-134. Natural Modes of Bernoulli-Euler Beams with Symmetric Cracks.
- [11] M. H. Shen and C. Pierre, *Journal of Sound and Vibration* submitted for publication, Free Vibrations of Beams with a Single-Edge Crack.
- [12] R. L. Crane, K. E. Hillstrom, and M. Minkoff 1980, ANL-80-64, Argonne National Laboratory, Argonne, Illinois. Solution of The General Nonlinear Programming Problem With Subroutine VMCON.

Test Data: $\xi_1^* = 0.84703$ , $\xi_3^* = 70.1348$ , $cr^* = 0.5$					
Initial Data			Final Data		
$\xi_1$	$\xi_3$	$cr$	$\xi_1$	$\xi_3$	$cr$
1.0	81.0	0.0	0.84684	70.1348	0.50033
0.98841	80.0769	0.1	0.84697	70.1346	0.50019
0.97217	78.8135	0.2	0.84704	70.1347	0.49998
0.94815	77.0062	0.3	0.84701	70.1348	0.50007
0.91032	74.3024	0.4	0.84694	70.1347	0.50024
0.73638	63.7848	0.6	0.84705	70.1348	0.49962
0.54574	55.0511	0.7	0.84703	70.1348	0.50034
0.27233	45.9316	0.8	0.84700	70.1347	0.50009

Table 1: Numerical results based on mean square problem statement of Eqs. (21-25) with the crack (damage) specified ( $zc = 0.5$ ).

Test Data: $\xi_1^* = 0.84703$ , $\xi_3^* = 70.1348$ , $cr^* = 0.5$ , $zc^* = 0.5$								
T	Initial Data				Final Data			
	$\xi_1$	$\xi_3$	$cr$	$zc$	$\xi_1$	$\xi_3$	$cr$	$zc$
9	0.91806	78.5161	0.4	0.4	0.69639	70.1359	0.99789	0.36289
9	0.91371	76.6365	0.4	0.43	0.70007	70.1362	0.99440	0.39620
9	0.91158	75.1335	0.4	0.46	0.84610	70.1347	0.91029	0.53775
9	0.91056	74.7464	0.4	0.47	0.84711	70.1347	0.67125	0.49033
9	0.91063	74.5157	0.4	0.48	0.84704	70.1348	0.50554	0.49972
9	0.73472	63.8062	0.6	0.51	0.84704	70.1348	0.60027	0.50526
9	0.73711	64.2643	0.6	0.52	0.84704	70.1348	0.60083	0.50531
9	0.73617	64.7619	0.6	0.53	0.84704	70.1348	0.60141	0.50534
9	0.73929	65.6727	0.6	0.54	0.84705	70.1348	0.60255	0.49459
9	0.73909	66.6112	0.6	0.55	0.84702	70.1348	0.99721	0.24709
9	0.75452	74.0109	0.6	0.6	0.70040	70.1363	0.99079	0.59307
45	0.97475	80.2193	0.2	0.4	0.90130	70.1347	0.94855	0.94404
45	0.91806	78.5161	0.4	0.4	0.84420	70.1345	0.53053	0.51586
45	0.91531	77.2676	0.4	0.42	0.84686	70.1347	0.50838	0.50198
45	0.96219	78.5819	0.25	0.45	0.84643	70.1348	0.51729	0.49389
45	0.75452	74.0109	0.6	0.6	0.84645	70.1348	0.51723	0.50609
45	0.64083	77.7173	0.7	0.7	0.89079	70.1347	0.58895	0.81817

Table 2: Numerical results based on mean square problem statement of Eqs. (21-25). The position of the damage  $zc$  is a variable.

Test Data: $\xi_1^* = 0.15296$ , $\xi_2^* = 1.2956$ , $\xi_3^* = 2.2494$ , $dm_1^* = 0.0$ , $dm_2^* = 0.5$ , $dm_3^* = 0.25$									
Initial Data					Final Data				
$\xi_1$	$\xi_2$	$dm_1$	$dm_2$	$dm_3$	$\xi_1$	$\xi_2$	$dm_1$	$dm_2$	$dm_3$
0.19806	1.5549	0.0	0.0	0.0	0.15299	1.2956	0.21392	0.40077	0.10985
0.18986	1.4975	0.0	0.1	0.05	0.15294	1.2955	0.17532	0.41741	0.13265
0.18123	1.4429	0.0	0.2	0.1	0.15296	1.2956	0.13478	0.43493	0.15777
0.17218	1.3911	0.0	0.3	0.15	0.15297	1.2956	0.09222	0.45445	0.18530
0.16275	1.3420	0.0	0.4	0.2	0.15293	1.2955	0.04751	0.47635	0.21576
0.15846	1.3088	0.0	0.44	0.24	0.15294	1.2956	0.02043	0.48975	0.23502
0.15494	1.3047	0.0	0.48	0.24	0.15295	1.2956	0.00973	0.49511	0.24281

Table 3: Numerical results for spring-mass model using first and second mode information.

Test Data: $\xi_1^* = 0.15296$ , $\xi_2^* = 1.2956$ , $\xi_3^* = 2.2494$ , $am_1^* = 0.0$ , $am_2^* = 0.5$ , $am_3^* = 0.25$											
Initial Data						Final Data					
$\xi_1$	$\xi_2$	$\xi_3$	$am_1$	$am_2$	$am_3$	$\xi_1$	$\xi_2$	$\xi_3$	$am_1$	$am_2$	$am_3$
0.19806	1.5549	3.2469	0.0	0.0	0.0	0.15294	1.2966	2.2494	0.0002	0.5001	0.2498
0.18986	1.4975	3.0209	0.0	0.1	0.05	0.15294	1.2953	2.2494	0.0002	0.5001	0.2498
0.18123	1.4429	2.8086	0.0	0.2	0.1	0.15242	1.2953	2.2494	0.0067	0.5026	0.2442
0.17218	1.3911	2.6095	0.0	0.3	0.15	0.15265	1.2953	2.2494	0.0039	0.5015	0.2494
0.16275	1.3420	2.4232	0.0	0.4	0.2	0.15280	1.2953	2.2494	0.0019	0.5008	0.2484
0.15848	1.3088	2.3329	0.0	0.44	0.24	0.15295	1.2956	2.2494	0.0000	0.5002	0.2499
0.15494	1.3046	2.2832	0.0	0.48	0.24	0.15292	1.2956	2.2494	0.0004	0.5002	0.2496

Table 4: Numerical results for spring-mass model using all three mode information.

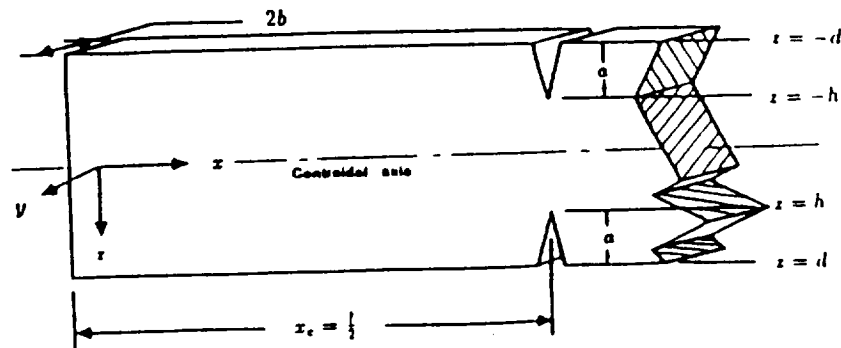


Figure 1: Geometry of a simply supported beam containing a pair of symmetric edge cracks at mid-span,  $x_c = l/2$ .

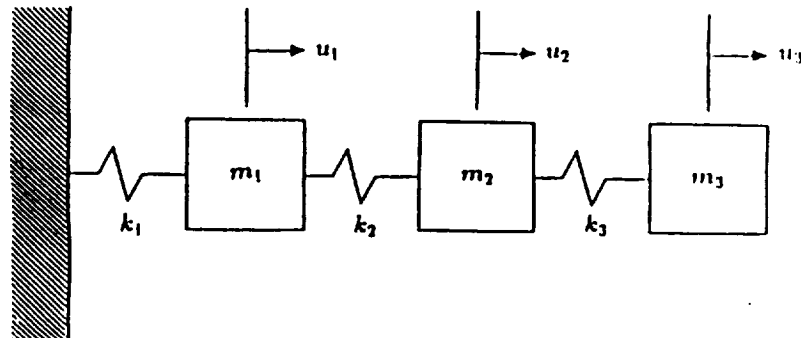


Figure 2: Geometry of a 3 DOF spring mass beam model

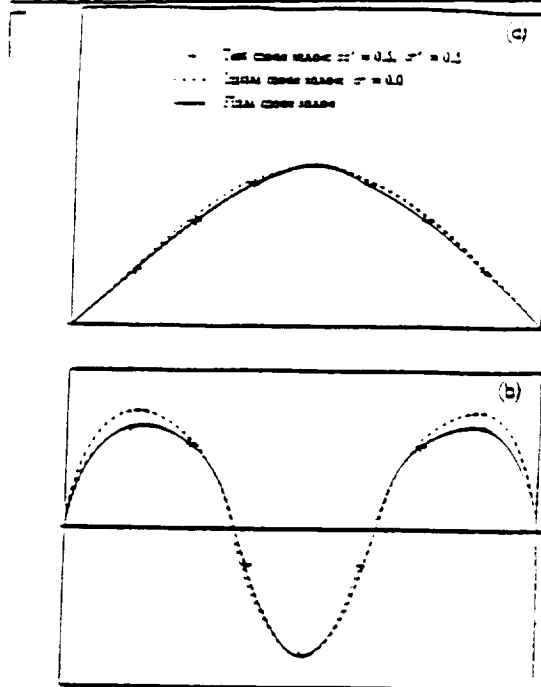


Figure 3. Comparison between the initial, final, and test mode shapes in the first model (a) and third model (b). The crack identification process is based on the least-square formulation with a specified crack position  $\alpha$  and 3 test stations. The beam is simply supported with symmetric cracks at mid-span, for  $\sigma^* = 1$ . The initial data is selected at  $\sigma^* = 0.0$ .

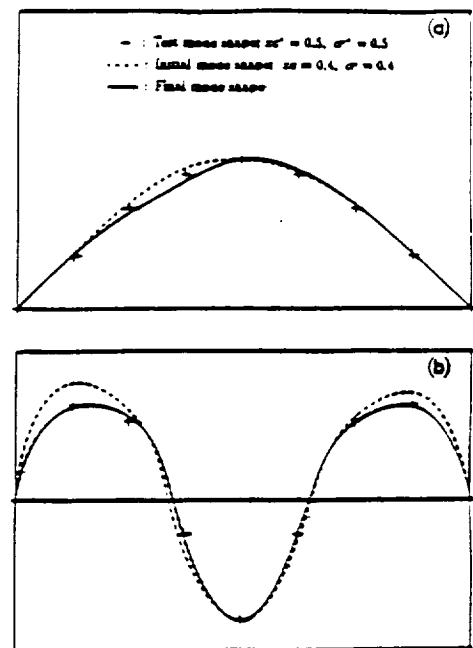


Figure 4. Comparison between the initial, final, and test mode shapes in the first model (a) and third model (b). The crack identification process is based on the least-square formulation, in which both crack position  $\alpha$  and crack ratio  $\sigma^*$  are unknown and 9 test stations. The beam is simply supported with symmetric cracks at mid-span, for  $\sigma^* = 1$ . The initial data is selected at  $\sigma^* = 0.4, \alpha = 0.4$ .

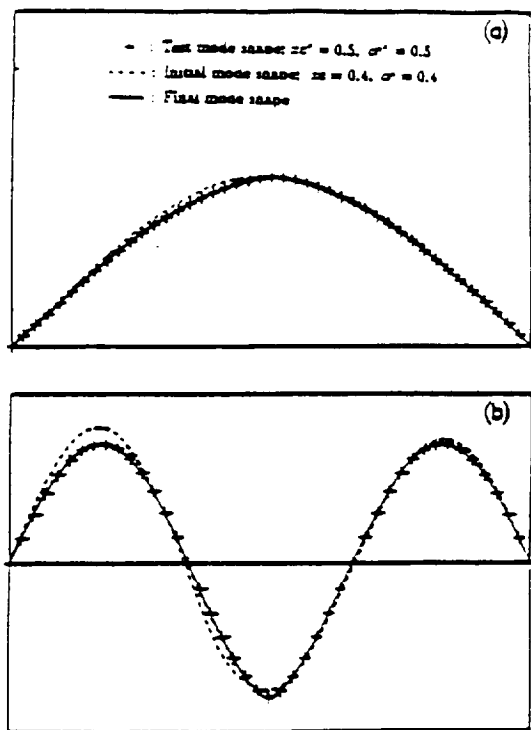


Figure 5. Comparison between the initial, final, and test mode shapes in the first model (a) and third model (b). The crack identification process is based on the least-square formulation in which both crack position  $\alpha$  and crack ratio  $\sigma^*$  are unknown and 45 test stations. The beam is simply supported with symmetric cracks at mid-span, for  $\sigma^* = 1$ . The initial data is selected at  $\sigma^* = 0.4, \alpha = 0.4$ .

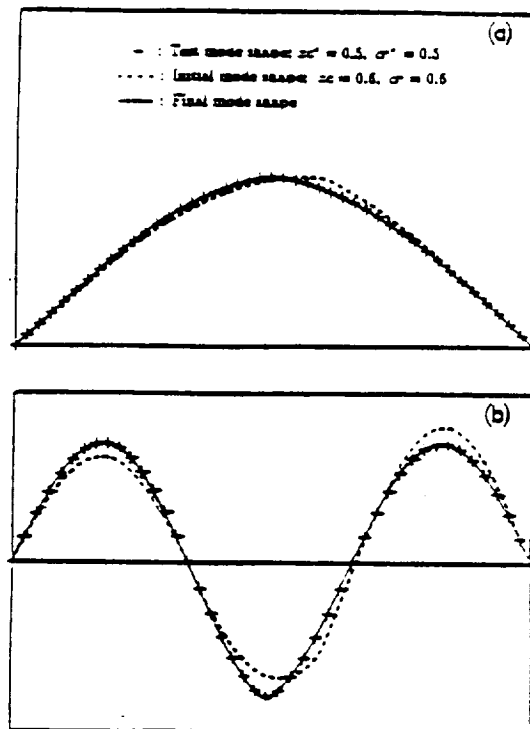


Figure 6. Comparison between the initial, final, and test mode shapes in the first model (a) and third model (b). The crack identification process is based on the least-square formulation in which both crack position  $\alpha$  and crack ratio  $\sigma^*$  are unknown and 45 test stations. The beam is simply supported with symmetric cracks at mid-span, for  $\sigma^* = 1$ . The initial data is selected at  $\sigma^* = 0.6, \alpha = 0.6$ .